

Hemodynamic Fingerprinting of Altered 3D Blood Characteristics in Aortic Disease

Julio Garcia¹, Alex J. Barker¹, Pim van Ooij¹, Susanne Schnell¹, S. Chris Malaisrie², Jeremy Collins¹, James Carr¹, and Michael Markl¹

¹Radiology, Northwestern University, Chicago, Illinois, United States, ²Division of Cardiac Surgery, Northwestern University, Chicago, Illinois, United States

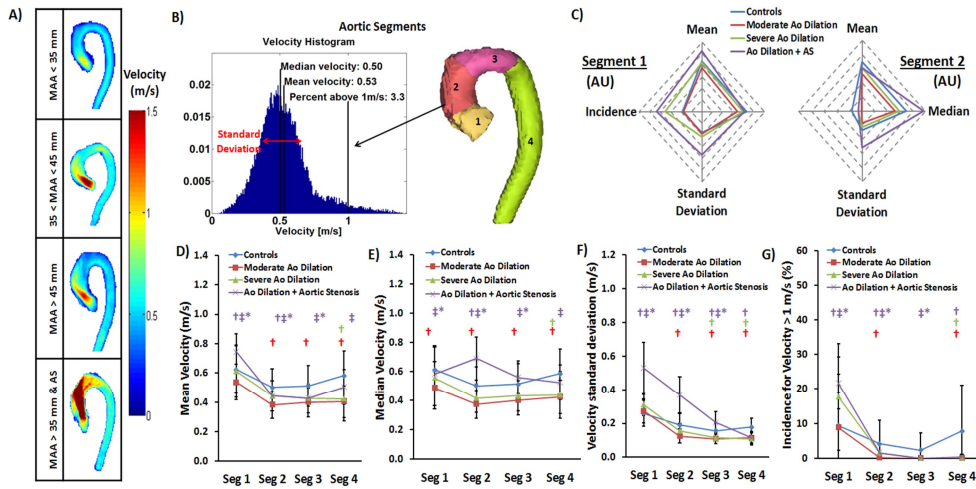


FIG. 1: Velocity distribution analysis. A) Time-resolved maximum intensity projection of the masked velocity field in an oblique-sagittal view for example patients from each group. B) Volumetric segmentation of the entire aorta and the regional segments used in the velocity distribution analysis. The velocity distribution for segment 2 is shown. C) Spider web plots provide a visual impression of the histogram characteristics for Segment 1 (left) and 2 (right). Plots are in arbitrary units (AU). D-G) Plots for the mean, median, standard deviation and incidence obtained from the velocity field analysis for each segment of the aorta as stratified by group. †: $p < 0.05$ with Controls; ‡: $p < 0.001$ with moderate Ao Dilation; *: $p < 0.001$ with severe Ao Dilation. Each symbol is color-coded to the corresponding group.

Purpose: Time-resolved 3D PC-MRI with three-directional velocity encoding (4D flow MRI) has been successfully applied in a number of studies for the analysis of altered hemodynamics in patients with cardiovascular disease¹. Data analysis, however, can be time consuming and often relies on the manual placement of 2D analysis planes at user defined vascular regions of interest. The analysis of flow parameters and derived metrics of hemodynamics are thus often limited by observer variability. In addition, the inherent volumetric 3D coverage of the vascular system of interest provided by 4D flow MRI is not fully utilized by analysis based on 2D planes. Nevertheless, a number of studies have shown that 4D flow MRI can detect the impact of vascular disease on changes in vascular hemodynamics. It was thus the aim of this study to evaluate a novel automated flow distribution analysis based on the evaluation the blood flow velocity distributions in the entire 3D vessel segments to identify hemodynamic ‘fingerprints’ of different aortic pathologies. Our goal was to test the feasibility of in-vivo hemodynamic fingerprinting to identify altered 3D flow characteristics in patients with aortic dilation and aortic valve stenosis without the need for the manual definition of 2D analysis planes.

Methods: 40 subjects (10 controls and 30 patients with aortic dilation and tricuspid aortic valves) (age=56±17 years, female=11) were identified via an IRB-approved retrospective chart review. The mid-ascending aorta (MAA) diameter was used to stratify by aortic (Ao) dilation and aortic valve peak velocity (PV) was used to determine the presence of aortic valve stenosis (AS). Each subject was classified into four groups: controls (n=10, MAA<35 mm and PV<1.5 m/s); moderate Ao dilation (n=10, 35<MAA<45 mm and PV<1.5 m/s); severe Ao dilation (n=10, MAA>45 mm and PV<1.5 m/s); Ao dilation + AS (n=10, MAA>35 mm and PV>1.5 m/s). 4D flow MRI was performed at 1.5T and 3T with full 3D coverage of the thoracic aorta (spatial resolution=2.5×2.1×3.2 mm³; temporal resolution=40-50 ms) using prospective ECG gating and a respiratory navigator gating. Pulse sequence parameters were as follows: 1.5 T scan parameters ranged from TE/TR=2.3-3.4/4.8-6.6 ms, flip angle $\alpha=7-15^\circ$ and a field of view of 340-400×200-300 mm; 3T scans used TE/TR =2.5/5.1 ms, flip angle $\alpha=7-15^\circ$, and a field of view of 400×308 mm. 3D PC-MR angiograms were computed and used to obtain a 3D segmentation of the aorta (Mimics, Materialise, Leuven, Belgium). Based on the segmentation, 4 aortic sub-regions were analyzed (see Fig. 1), including: Segment 1, traversing the left ventricle outflow tract to the sinotubular junction; Segment 2, which progresses from the sino-tubular junction to the aortic arch; Segment 3, which covers the aortic arch; and Segment 4, which includes the proximal descending aorta. The four vascular 3D segments were used to compute a masked 4D velocity field (3 spatial dimensions + time) for each aortic segment. The masked aorta velocity field was used to generate a time-resolved maximum intensity projection (MIP) in an oblique sagittal plane using the three peak systolic velocity phases, Fig. 1A. The velocities for all voxels and cardiac time-frames inside an aortic segment were plotted in histogram form and normalized by the total number of voxels in order to create a cohort-specific hemodynamic fingerprint that can be compared across subjects and cohorts. In addition, mean, median, standard deviation, and the normalized number of voxels >1m/s (incidence) were calculated as shown in Fig. 1B for Segment 2 (Matlab, Natick, MA, USA). A sensitivity analysis was conducted to identify which proportions of the velocity distribution (number of time frames and top % of velocities) were most sensitive to differences in flow distribution between patient groups and controls. At each threshold, a t-test was conducted to evaluate the significance of difference between groups and it was determined that the first 8 time steps of the cardiac cycle (320-400ms) and 100% of the data were optimal for the detection of cohort differences.

Table 1

	Subject Characteristics				
	All	Controls	Moderate Ao Dilation	Severe Ao Dilation	Ao Dilation + Aortic Stenosis
n	40	10	10	10	10
Age	58 ± 16	41 ± 16	63 ± 11 †	62 ± 10 †	64 ± 14 †
Female (n)	11	2	4	4	1
Stroke Volume (mL)	93 ± 30	85 ± 13	84 ± 21	100 ± 47	102 ± 26
Sinus of Valsalva Diameter (mm)	41 ± 5	39 ± 9	41 ± 3	42 ± 5	39 ± 4
Mid Ascending Aorta Diameter (mm)	40 ± 7	30 ± 4	41 ± 3 †	47 ± 2 †	42 ± 3 †*
Peak Velocity (m/s)	1.7 ± 0.9	1.2 ± 0.4	1.3 ± 0.3	1.4 ± 0.5	2.9 ± 0.9 ††*

†: $p < 0.05$ with Controls; ‡: $p < 0.001$ with Moderate Ao Dilation; *: $p < 0.001$ with Severe Ao Dilation.

differences may be due to the severity of Ao dilation and helical flow in groups with Ao dilation. For almost all segments, the velocity standard deviation was significantly higher for Ao Dilation+AS vs. other groups (Fig. 1E). The incidence for velocities > 1 m/s was significantly increased for Ao Dilation+AS in segment 1 due to valve stenosis.

Discussion: The volumetric velocity distribution analysis presented here has demonstrated: 1) 3D blood flow velocity distributions may identify hemodynamic fingerprints of different aortic pathologies via basic statistical descriptors (i.e. mean, median, standard deviation and incidence), and 2) the characterization of hemodynamic fingerprints along regional aortic segments in subjects with aortic disease. The automatic distribution analysis of 4D flow data may be useful in the automated characterization of hemodynamic ‘fingerprinting’ of cardiovascular disease by identifying simple characteristic parameters associated with the presence of pathology. The results indicate a selection of blood flow behaviours which are capable of stratifying the presence of disease, as shown for Ao Dilation+AS group.

Conclusion: The systematic velocity distribution analysis of 4D flow velocity data may identify fingerprint characteristic of blood flow patterns in aortic diseases. Further studies are needed to evaluate the association of velocity distribution derived descriptors with patient outcome.

Acknowledgment: Grant support by NIH R01HL115828, AHA 13SDG14360004, CONACyT postdoctoral fellow grant (223355).

References: 1. Markl M et al. J Magn Res Imaging 2012; 36:1015-36.

Results: Subject characteristics are summarized in Table 1. All subjects had normal ejection fraction (60±7%), although severe Ao Dilation was significantly elevated ($p < 0.05$ vs. Controls). Examples of velocity MIPs in Fig. 1A visually illustrate disease specific differences in the aortic velocity patterns and distribution. The appearance of the patient flow patterns, as seen in the velocity MIPs, were heterogeneous compared to controls. The dilated aortas displayed outflow jets and high flow regions (red color) which were most pronounced for the AS patients. Examples of spider web plots for flow parameter fingerprints are shown in Fig. 1C, which provide a visual impression of the flow characteristics. The velocity histogram parameters are shown in Fig. 1C-F. The mean velocity for Ao Dilation+AS was significantly different from other groups in all segments due to aortic stenosis, Fig. 1C. Interestingly for median velocities, Segment 2 showed a significant difference between moderate Ao Dilation and Ao Dilation+AS, Fig. 1D. These differences were most pronounced for the AS patients. Examples of spider web plots for flow parameter fingerprints are shown in Fig. 1C, which provide a visual impression of the flow characteristics. The velocity histogram parameters are shown in Fig. 1C-F. The mean velocity for Ao Dilation+AS was significantly different from other groups in all segments due to aortic stenosis, Fig. 1C. Interestingly for median velocities, Segment 2 showed a significant difference between moderate Ao Dilation and Ao Dilation+AS, Fig. 1D. These differences were most pronounced for the AS patients.